Phase diagram of the electronic states of trilayered ruthenate $Sr_4Ru_3O_{10}$

D. Fobes,[1] M. H. Yu,[2] M. Zhou,[1] J. Hooper,[1] C. J. O'Connor,[2] M. Rosario,[3] and Z. Q. Mao[1,*]
[1]*Department of Physics, Tulane University, New Orleans, Louisiana 70118, USA*
[2]*Advanced Materials Research Institute, University of New Orleans, New Orleans, Louisiana 70148, USA*
[3]*Department of Physics and Astronomy, Saint Mary's College of California, Moraga, California 94575, USA*
(Received 19 December 2006; published 27 March 2007)

Trilayered ruthenate $Sr_4Ru_3O_{10}$ exhibits an interesting itinerant metamagnetic transition for magnetic fields applied along in-plane directions. Our earlier work has revealed that this metamagnetic transition occurs via a phase separation process with magnetic domain formation [Z. Q. Mao *et al.*, Phys. Rev. Lett. **96**, 077205 (2006)]. We recently performed systematic investigations on its magnetotransport properties and constructed a magnetic field–temperature (*H-T*) phase diagram. In the phase separated regime of the phase diagram, due to domain boundary scattering, the resistivity is increased and shows nonmetallic temperature dependence, while outside the phase separation regime, the system shows Fermi-liquid ground-state properties, i.e., $\rho \propto T^2$. The Fermi-liquid temperature is strongly suppressed near the metamagnetic transition. The transport properties in the mixed phase region are sensitive to the disorders, and the magnetoresistivity steps in this region are found to be suppressed by increasing the level of disorders. In addition, we discussed the possible mechanism of the metamagnetic transition of this material.

DOI: 10.1103/PhysRevB.75.094429 PACS number(s): 75.30.Kz, 71.27.+a, 75.47.−m, 75.60.Ch

I. INTRODUCTION

Ruddlesden-Popper (RP) series strontium ruthenates $Sr_{n+1}Ru_nO_{3n+1}$ exhibit a rich variety of fascinating ground-state properties, such as spin-triplet superconductivity in Sr_2RuO_4 ($n=1$),[1–3] metamagnetic quantum criticality in $Sr_3Ru_2O_7$ ($n=2$),[4–6] and itinerant ferromagnetism in $SrRuO_3$ ($n=\infty$).[7,8] Studies on these diverse ground-state properties advance our understanding of the physics of strongly correlated electron systems. $Sr_4Ru_3O_{10}$, the material studied in this paper, is the $n=3$ member of the RP series with triple layers of corner shared RuO_6 octahedra in its unit cell. Previous magnetization measurements and structure studies suggested that this material is a structurally distorted ferromagnet with a Curie temperature $T_C=105$ K,[9,10] which has recently been confirmed by a neutron scattering experiment.[11] This material exhibits complex magnetic behaviors under magnetic fields.[9,10] For magnetic fields applied along the *c* axis, it exhibits characteristics consistent with a typical ferromagnet. However, for fields applied along the in-plane direction, the ferromagnetic transition is followed by an additional magnetic transition at 50 K and the magnetic susceptibility shows a pronounced peak at this temperature. Below this temperature, a field sweep of magnetization shows a superlinear increase at a characteristic field (about 2 T for $T=2$ K), which can empirically be defined as a metamagnetic transition.[9,10] This metamagnetic transition is strongly first order, exhibiting significant hysteresis upon downward field sweeps.

The metamagnetic transition in $Sr_4Ru_3O_{10}$ exhibits intriguing features: (1) This transition occurs via a phase-separation process with magnetic domain formation, which results in ultrasharp magnetoresistivity steps.[12] (2)The transition is accompanied by a significant change in the B_{1g} phonon frequency (which is associated with internal vibrations of the RuO_6 octahedra), demonstrating a distinct structural contribution to the metamagnetic transition.[13] (3) As the magnetic field rotates away from the *ab* plane, the transition bifurcates into two transitions.[14] One transition occurs below 1 T and corresponds to the ferromagnetic response, while the other transition, corresponding to the metamagnetic response, shifts to a higher field. Such a coexistence of ferromagnetic and metamagnetic behaviors implies a multiple-band effect.[14] All of these features suggest that $Sr_4Ru_3O_{10}$ is a good candidate for the study of physics associated with metamagnetic behavior, electronic inhomogeneity, orbital dependence of magnetism, and spin-lattice coupling. In this paper, we report a magnetic field–temperature (*H-T*) phase diagram of the electronic state of $Sr_4Ru_3O_{10}$, which is constructed from systematic electronic transport property measurements.

II. EXPERIMENT

Our crystals were grown by floating-zone technique.[15] Crystals selected for the measurements were well characterized by x-ray diffraction and were found to be pure $Sr_4Ru_3O_{10}$. Our measurements were carried out with a physical property measurement system (PPMS, Quantum Design) and a He^3 cryostat with a base temperature of 0.3 K, using a standard four-probe technique. The transport data presented in Figs. 1–3 were obtained from a crystal with residual resistivity of $\rho_0=6.2$ $\mu\Omega$ cm, which was used previously.[12]

III. RESULTS AND DISCUSSION

Figure 1 shows the temperature dependence of in-plane resistivity $\rho_{ab}(T)$ under various magnetic fields applied parallel to the *ab* plane for an upward field sweep. $\rho_{ab}(T)$ shows a sharp change across the metamagnetic transition. At fields below the transition, $\rho_{ab}(T)$ exhibits T^2 dependence, a typical behavior of a Fermi-liquid ground state [see Fig. 1(a) inset]. For fields above the transition, we also observe T^2 dependence in $\rho_{ab}(T)$, but it occurs only in a very low temperature

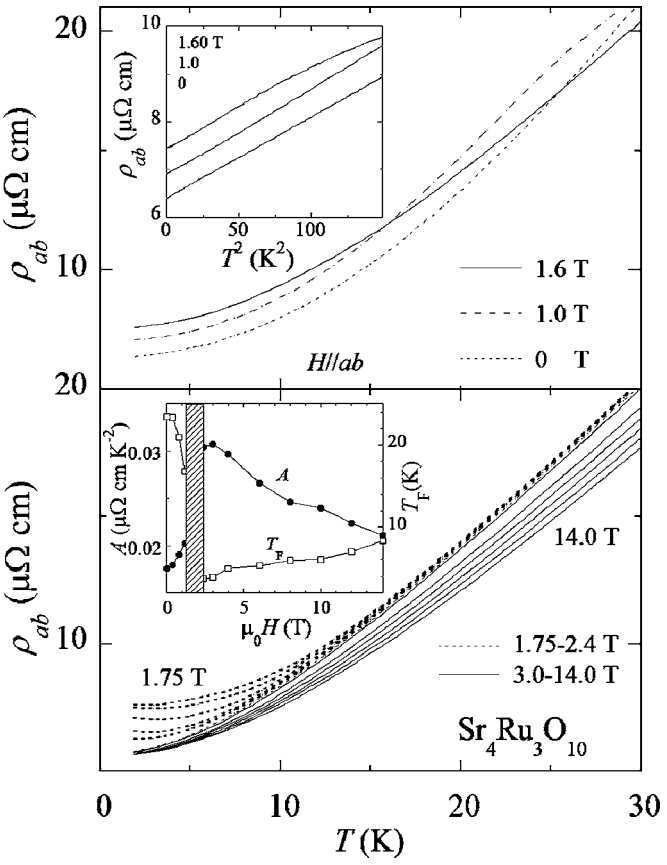

FIG. 1. In-plane resistivity ρ_{ab} as a function of temperature under various applied magnetic fields for an upward field sweep (a) below the metamagnetic transition and (b) within and above the transition. Inset (a): T^2 dependence of the in-plane resistivity below the transition. Inset (b): Fermi-liquid temperature T_F (right) and the coefficient of the temperature-dependent term A in resistivity (left) as a function of applied field $H_{\|ab}$, extracted from fitting the experimental data to $\rho=\rho_0+AT^2$.

range: $\rho_{ab}(T)\propto T^{5/3}$ for higher temperatures.[12] However, for fields close to the transition, $\rho_{ab}(T)$ no longer shows the T^2 behavior [see the dashed curves in Fig. 1(b)], instead a nonmetallic behavior develops in the low-temperature region near the middle of the transition. This nonmetallic behavior becomes much more remarkable when temperature is below 2 K (see our previously reported data[12]). Another striking feature seen in the transition range is that ρ_{ab} at given temperatures remains approximately constant as the field increases for $T>15$ K, but shows a divergent behavior for $T<15$ K. This behavior is in sharp contrast to the observation for the fields above the transition, where ρ_{ab} tends to converge at lower temperatures.

We fitted the resistivity data to the formula $\rho=\rho_0+AT^2$ for the fields outside the transition region to derive the coefficient A of the temperature-dependent term of resistivity and the Fermi-liquid temperature T_F, below which $\rho_{ab}(T)$ follows a quadratic temperature dependence. The inset of Fig. 1(b) shows the dependence of A and T_F on the applied magnetic field. Consistent with the metamagnetic behavior seen in the related material $Sr_3Ru_2O_7$,[4] when the applied magnetic field approaches the metamagnetic transition field, T_F is suppressed and A tends to increase,[22] suggesting the presence of metamagnetic quantum critical fluctuations. Nevertheless, these fluctuations should be much weaker than those seen in

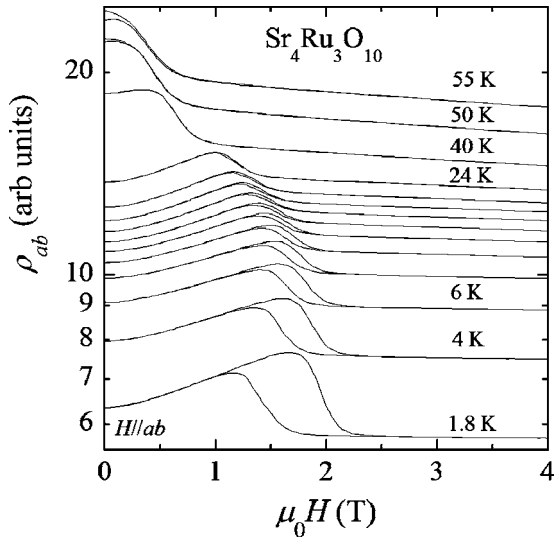

FIG. 2. Magnetic field dependences of the in-plane resistivity ρ_{ab} at various temperatures. Temperatures are 1.8, 4, 6, 8, 10, 12, 14, 16, 18, 20, 24, 40, 50, and 55 K. Data have been shifted for clarity. B_{C2} is defined as the upper critical field of the transition for an upward field sweep, above which the magnetoresistivity is saturated and the hysteresis starts below B_{C2} in a downward field sweep. B_{C2}' is defined as the lower critical field of the transition for a downward field sweep, below which the hysteres is terminates.

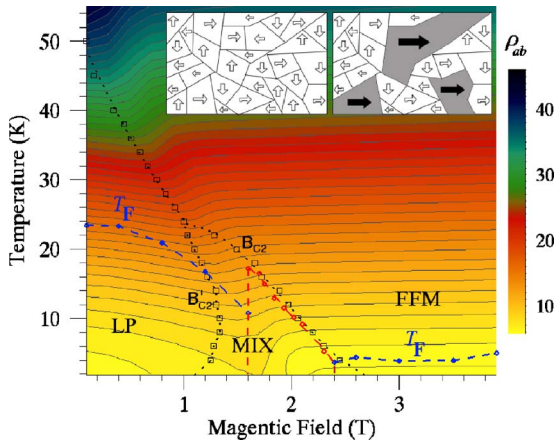

FIG. 3. (Color online) Contour plot of in-plane resistivity as a function of magnetic field ($\|$ *ab* plane, upward sweep) and temperature. LP, lowly polarized phase; FFM, forced ferromagnetic phase; MIX, mixed phase [the area enclosed by the dotted lines $B_{C2}(T)$ and $B_{C2}(T)'$]; B_{c2}, the upper critical field of the metamagnetic transition for an upward field sweep; B_{C2}', the lower critical field of the transition for a downward field sweep; and T_F, Fermi-liquid temperature. For B_{C2} and B_{C2}' the square-shaped symbols are data points and the dotted lines are visual guides. Left inset illustrates ferromagnetic domains in the uniform LP phase; right inset shows the coexistence of the ferromagnetic domains of the LP phase and FFM domains (marked by black arrows). The ferromagnetic domains are intrinsically different from the FFM domains (see the text).

$Sr_3Ru_2O_7$.[12] For magnetic fields within the metamagnetic transition range where the resistivity data could not be fitted with $\rho=\rho_0+AT^2$ [the shadowed region in the inset of Fig. 1(b)], $Sr_4Ru_3O_{10}$ exhibits different properties from $Sr_3Ru_2O_7$. In $Sr_3Ru_2O_7$ quantum fluctuations dominate the transport properties in the transition region, which gives rise to a non-Fermi-liquid behavior, i.e., a linear temperature dependence in $\rho(T)$, while in $Sr_4Ru_3O_{10}$ the metamagnetic transition occurs via a phase-separation process with magnetic domain formation, and the domain boundary scattering results in the presence of the nonmetallic behavior in resistivity.[12] It is worth pointing out that recent experiments on ultrapure crystals of $Sr_3Ru_2O_7$ reveal a different phase below 1 K, in close proximity to the metamagnetic quantum critical end point, and that this phase exhibits a weak nonmetallic temperature dependence in resistivity.[6] Although this behavior appears to be similar to our observation in $Sr_4Ru_3O_{10}$, its origin might be different, possibly due to a spin-dependent symmetry-breaking Fermi-surface distortion.

Figure 2 shows the magnetic-field dependences of the in-plane resistivity $\rho_{ab}(H)$ at various temperatures. Consistent with the previously reported data,[10] the metamagnetic transition shifts to a lower field as the temperature increases and it disappears at about 50 K. As indicated above, the metamagnetic transition in $Sr_4Ru_3O_{10}$ exhibits a marked hysteresis upon a downward field sweep. This hysteresis is also strongly temperature dependent; it weakens dramatically with increasing temperature and becomes unobservable as the temperatures reach about 25 K. Interestingly, when the temperature is above 50 K, the downward field sweep leads to a small hysteresis at low field. Apparently, this hysteresis is a generic behavior of ferromagnets, which is intrinsically different from the metamagnetic hysteresis seen below 25 K. More discussions for this will be given below.

Figure 3 shows the magnetic field–temperature (H-T) phase diagram of $Sr_4Ru_3O_{10}$, which is constructed according to a contour plot of in-plane resistivity as a function of temperature and magnetic field measured in an upward field sweep. The metamagnetic transition field is marked by the dotted lines B_{C2} and B_{C2}' in the diagram. B_{C2} represents the upper critical field determined from the upward field sweeps of resistivity; it is defined as the field above which the magnetoresistivity saturates. To identify the phase separation region in the diagram, we also added the lower critical field B_{C2}' measured in the downward field sweeps of resistivity to Fig. 3. The definitions of B_{C2} and B_{C2}' are shown in Fig. 2. The Fermi-liquid temperatures T_F shown in the inset of Fig. 1 are also included in this diagram. As seen in Fig. 3, B_{C2} overlaps with B_{C2}' for temperatures above 25 K. The regime between B_{C2} and B_{C2}' for $T<25$ K marks the field range where hysteresis occurs. In our earlier paper,[12] we reported that the magnetoresistivity exhibits ultrasharp steps in this field range for a downward field sweep. Our analysis given there indicated that these magnetoresistivity steps originate from a phase-separation process with magnetic domain formation. While the magnetoresistivity steps occur only below 1 K as shown in Fig. 4, the hysteresis between B_{C2} and B_{C2}' below 25 K should all be associated with the magnetic domain formation and motion as discussed below. Therefore,

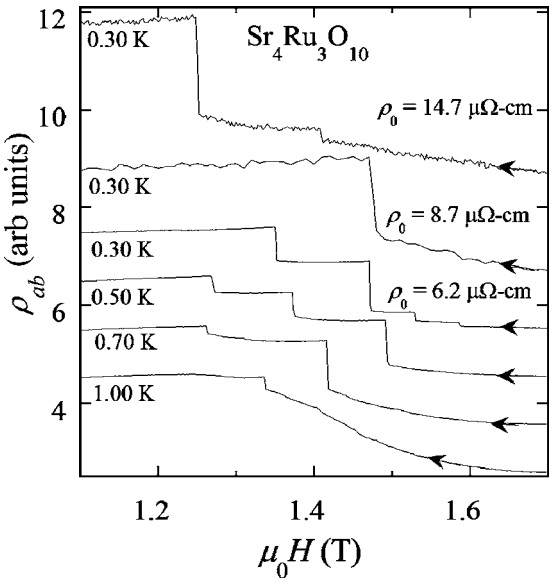

FIG. 4. Downward field sweep of in-plane resistivity ρ_{ab} for $H_{\|ab}$ for samples with different residual resistivities ρ_0. Also shown is the temperature dependence of the number of steps for the $\rho_0=6.2$ $\mu\Omega$ cm sample. Data have been shifted for clarity.

we define the area between B_{C2} and B_{C2}' in the phase diagram as the phase-separated regime. Here we use the same notations as used in our earlier paper[12] to describe the phases outside the metamagnetic transition region: the phase below B_{C2}' is denoted by LP (the lowly polarized phase) and the phase above B_{C2} is denoted by FFM (the forced ferromagnetic phase). Thus the area between B_{C2} and B_{C2}' can be represented by the mixture of LP and FFM phases. In an upward field sweep, the metamagnetic transition occurs through the formation of FFM domains, while in a downward, field sweep, the transition occurs via the formation of LP domains (see the schematic in Fig. 4 of our early paper[12]).

The mixed phase is dramatically different from the uniform LP phase below B_{C2}' or the FFM phase above B_{C2} in transport properties. As seen in Fig. 3, the contour line minimum occurring in the phase-separated region indicates that the mixed phase has increased resistivity. The phase-separated region can further be split into two subregions (separated by the vertical red dashed line at 1.6 T). The left subregion shows a quadratic temperature dependence in resistivity as the uniform LP phase, but the Fermi-liquid temperature T_F in this region is strongly suppressed in comparison with the uniform LP phase. This observation suggests that although FFM domains form in this region, the number of domains, as well as the domain size, is not substantially large and the domain-boundary scattering does not make critical contribution to the transport properties. However, for the right subregion marked by red dashed lines, the resistivity no longer shows quadratic temperature dependence and nonmetallic behavior develops in the low-temperature region for the fields close to 1.8 T.[12] The red circles in this region represent the temperatures where $d\rho(T)/dT$ shows a sharp change. The variation of this characteristic temperature with the field coincides well with the phase boundary of $B_{C2}(T)$,

which is determined from the field sweep of resistivity. As we discussed previously,[12] both the increased resistivity and the nonmetallic behavior observed in this region can be ascribed to the domain-boundary scattering. The low-temperature divergent behavior in ρ_{ab} for $1.75\ \mathrm{T} < \mu_0 H < 2.5\ \mathrm{T}$ mentioned above [see Fig. 1(b)] is clearly due to the same origin, while the low-temperature convergent behavior of ρ_{ab} for $\mu_0 H > 2.5$ T is due to the formation of precolative network of FFM phase, which has lower resistivity and dominates the transport properties.[12]

The transport properties in the mixed phase region are very sensitive to the disorders in the sample; this can be seen from Fig. 4, which shows the field dependence of in-plane resistivity within the mixed phase region for three samples with different levels of disorder. The sample with $\rho_0 = 6.2\ \mu\Omega$ cm, which is used for the construction of the phase diagram and should have less disorder, shows four magnetoresistivity steps, while the other two samples with higher residual resistivity, which should have higher disorder levels, exhibit only one or two steps. According to our previous discussions,[12] the magnetoresistivity steps in $Sr_4Ru_3O_{10}$ stem from the formation of continuous domain walls of the LP phase at certain threshold fields in the downward field sweep. Thus our observation of the suppression of magnetoresistivity steps by disorders suggests that the disorder plays a critical role in the domain formation throughout the metamagnetic transition of $Sr_4Ru_3O_{10}$. Further work is necessary to understand how the disorders affect the domain formation.

Magnetic domain formation in itinerant metamagnets has recently been investigated theoretically by Binz *et al.*[16] They generalized the theory of Condon domains[17] to the case of itinerant metamagnets and considered a model for a specific two-dimensional electron system whose Fermi level is close to a Van Hove singularity. Their results indicated that an itinerant electron system cannot undergo a first-order transition without breaking up into magnetic domains within a finite range of applied fields and that magnetic domain formation in itinerant metamagnets is driven by dipolar magnetostatic force. This theoretical prediction is quite consistent with our experimental observation in $Sr_4Ru_3O_{10}$. Moreover, the qualitative similarities between the theoretical phase diagram and our experimentally established phase diagram in Fig. 3 are striking. However, it is currently unclear whether the domains we observed in $Sr_4Ru_3O_{10}$ have the characteristics of Condon domains as expected in their theory. Further experiments are needed to clarify the nature of magnetic domains in $Sr_4Ru_3O_{10}$.

Next let us examine the mechanism of the metamagnetic transition in $Sr_4Ru_3O_{10}$. In general, itinerant metamagnetism can be interpreted as a field-tuned Stoner transition into a highly polarized magnetic state[4,16] or the suppression of antiferromagnetic correlations.[18] Recent experiments on the Shubnikov–de Haas (SdH) effect of $Sr_4Ru_3O_{10}$ reveal a nontrivial evolution of the geometry of the Fermi surface and an enhancement of the quasiparticle effective mass across the metamagnetic transition when the applied field is aligned close to the *c* axis, where the metamagnetic transition field is shifted to above 30 T.[14] This result supports the assumption that the metamagnetic transition in $Sr_4Ru_3O_{10}$ is likely due to the field-tuned Stoner transition as in $Sr_3Ru_2O_7$. Since the magnetic ground state of $Sr_4Ru_3O_{10}$ at zero field is ferromagnetic, which is in contrast to the paramagnetic state in $Sr_3Ru_2O_7$, the field-tuned Stoner transition in $Sr_4Ru_3O_{10}$ can be understood only in terms of a multiple-band effect, i.e., both ferromagnetic and metamagnetic bands coexist in $Sr_4Ru_3O_{10}$.

Within the above framework of orbital-dependent magnetism, complex magnetic behavior of $Sr_4Ru_3O_{10}$ under magnetic fields can be understood. As indicated above, the magnetic susceptibility shows a peak at 50 K for $H \| ab$ plane. However, both specific heat[19] and neutron-scattering measurements[11] do not show any evidence that this peak is associated with any extra magnetic ordering. We think that this transition might be due to the formation of a special form of ferromagnetic domains. According to the neutron-scattering experiment,[11] the magnetic moments in $Sr_4Ru_3O_{10}$ are aligned in the basal plane. Magnetic moments in each domain below 50 K probably point to four different equivalent easy directions in the plane; thus magnetization is cancelled among domains below 50 K, which gives rise to a peak in susceptibility at 50 K. The presence of such domains minimizes magnetic self-energy. The left inset in Fig. 3 shows the schematic of such ferromagnetic domains. The uniform LP phase in the phase diagram should have such ferromagnetic domains. These domains can be easily polarized along the *c* axis, but not along the in-plane direction because of its strong in-plane magnetocrystalline anisotropy [which can be assumed to be comparable to that of the related material $SrRuO_3$ that has an internal crystalline anisotropy field of about 2 T (Ref. 20)]. Thus we can understand why the magnetization show typical ferromagnetic behaviors for $H \| c$ and a metamagnetic transition for $H \| ab$. The disappearance of the ferromagnetic hysteresis at lower field (below 1 T) for temperatures below 50 K (see Fig. 2) can also be explained in this picture: when the applied field is below the metamagnetic transition region, the ferromagnetic domains are rigid and cannot be driven by the applied field because of the strong in-plane magnetocrystalline anisotropy. This interpretation implies that the in-plane magnetocrystalline anisotropy in $Sr_4Ru_3O_{10}$ is temperature dependent and it intensifies considerably below 50 K; this conjecture is consistent with the observation in $SrRuO_3$, where the crystal anisotropy was indeed found to strongly increase below 48 K.[20,21]

As the field approaches the metamagnetic transition field, ferromagnetic domains will flip or flop to the direction of applied field in a phase-separated form, as shown schematically in the right inset of Fig. 3. It should be emphasized here that this local domain flip or flop transition in $Sr_4Ru_3O_{10}$ cannot be viewed as a regular ferromagnetic domain alignment under magnetic field. Since $Sr_4Ru_3O_{10}$ has strong magnetoelastic coupling[13] when ferromagnetic domains are aligned along the direction of applied field, the internal field would increase drastically, which subsequently drives the metamagnetic bands to polarized states. This point of view strongly supports the following experimental observations: First, the evidence for the Fermi-surface reconstruction across the metamagnetic transition of $Sr_4Ru_3O_{10}$ has been observed in SdH effect as indicated above. Second, Raman

spectra measurements indicate that the metamagnetic transition in $Sr_4Ru_3O_{10}$ involves a distinct structural contribution.[13] Third, a sharp peak in specific heat has recently been observed near the transition.[19] All these features cannot be understood only in terms of regular ferromagnetic domain reorientation. The gray areas (i.e., FFM domains) denoted by black arrows in the right inset of Fig. 3 describe that the metamagnetic transition occurs only in those areas where ferromagnetic domains flip or flop to the field direction. Either FFM domains in an upward field sweep or LP domains in a downward field should be much bigger than the ferromagnetic domains.

IV. CONCLUSION

In conclusion, we constructed a magnetic field–temperature phase diagram describing the electronic ground state of $Sr_4Ru_3O_{10}$. We found that by using magnetic field as a tuning parameter, the ground-state transitions from a uniform lowly polarized state to a mixed lowly polarized or highly polarized state, and then to a uniform highly polarized state. In the mixed phase region, the domain-boundary scattering plays a critical role in transport properties. It is responsible for the nonmetallic behavior in resistivity observed in an upward field sweep and the ultrasharp magnetoresistivity steps seen in a downward field sweep. The transport properties in the mixed phase region are found to be sensitive to disorders; the increase of disorder level suppresses the magnetoresistivity steps. In addition, we discussed the possible origin of the metamagnetic transition in $Sr_4Ru_3O_{10}$ in terms of our data and other related experiments. We argued that the metamagnetic transition in $Sr_4Ru_3O_{10}$ involves a multiple-band effect. Both ferromagnetic and metamagnetic bands coexist in these materials. Further work needs to be performed to gain a further understanding of the complex orbital-dependent magnetism involved in this material.

ACKNOWLEDGMENTS

We would like to thank W. Bao, L. Balicas, M. Salamon, B. Binz, and Y. Liu for useful discussions. This work was supported by the Louisiana Board of Regents support fund LEQSF(2003-06)-RD-A-26 at Tulane and DARPA Grant No. MDA972-02-1-0012 at UNO. Z.Q.M. thanks the Research Corporation for financial support.

*Electronic address: zmao@tulane.edu

[1] K. Ishida, H. Mukuda, Y. Kitaoka, K. Asayama, Z. Q. Mao, Y. Mori, and Y. Maeno, Nature (London) **396**, 658 (1998).
[2] A. Mackenzie and Y. Maeno, Rev. Mod. Phys. **75**, 657 (2003).
[3] K. D. Nelson, Z. Q. Mao, Y. Maeno, and Y. Liu, Science **306**, 1151 (2004).
[4] R. S. Perry, L. M. Galvin, S. A. Grigera, L. Capogna, A. J. Schofield, A. P. Mackenzie, M. Chiao, S. R. Julian, S. I. Ikeda, S. Nakatsuji, Y. Maeno, and C. Pfleiderer, Phys. Rev. Lett. **86**, 2661 (2001).
[5] S. A. Grigera, R. S. Perry, A. J. Schofield, M. Chiao, S. R. Julian, G. G. Lonzarich, S. I. Ikeda, Y. Maeno, A. J. Millis, and A. P. Mackenzie, Science **294**, 329 (2001).
[6] S. A. Grigera, P. Gegenwart, R. A. Borzi, F. Weickert, A. J. Schofield, R. S. Perry, T. Tayama, T. Sakakibara, Y. Maeno, A. G. Green, and A. P. Mackenzie, Science **306**, 1154 (2004).
[7] P. B. Allen, H. Berger, O. Chauvet, L. Forro, T. Jarlborg, A. Junod, B. Revaz, and G. Santi, Phys. Rev. B **53**, 4393 (1996).
[8] L. Klein, J. S. Dodge, C. H. Ahn, G. J. Snyder, T. H. Geballe, M. R. Beasley, and A. Kapitulnik, Phys. Rev. Lett. **77**, 2774 (1996).
[9] M. K. Crawford, R. L. Harlow, W. Marshall, Z. Li, G. Cao, R. L. Lindstrom, Q. Huang, and J. W. Lynn, Phys. Rev. B **65**, 214412 (2002).
[10] G. Cao, L. Balicas, W. H. Song, Y. P. Sun, Y. Xin, V. A. Bondarenko, J. W. Brill, S. Parkin, and X. N. Lin, Phys. Rev. B **68**, 174409 (2003).
[11] W. Bao, Z. Mao, M. Zhou, J. Hooper, J. Lynn, R. Freitas, P. Schiffer, Y. Liu, H. Yuan, and M. Salamon, cond-mat/0607428 (to be published).
[12] Z. Q. Mao, M. Zhou, J. Hooper, V. Golub, and C. J. O'Connor, Phys. Rev. Lett. **96**, 077205 (2006).
[13] R. Gupta, M. Kim, H. Barath, S. L. Cooper, and G. Cao, Phys. Rev. Lett. **96**, 067004 (2006).
[14] Y. Jo, L. Balicas, N. Kikugawa, K. Storr, M. Zhou, and Z. Mao, cond-mat/0605504 (to be published).
[15] M. Zhou, J. Hooper, D. Fobes, Z. Mao, V. Golub, and C. O'Connor, Mater. Res. Bull. **40**, 942 (2005).
[16] B. Binz, H. B. Braun, T. M. Rice, and M. Sigrist, Phys. Rev. Lett. **96**, 196406 (2006).
[17] J. Condon, Phys. Rev. **145**, 526 (1966).
[18] E. Stryjewski and N. Giordano, Adv. Phys. **26**, 487 (1977).
[19] G. Cao, S. Chikara, J. Brill, and P. Schlottmann, cond-mat/0605734 (to be published).
[20] A. Kanbayasi, J. Phys. Soc. Jpn. **44**, 89 (1978).
[21] A. Kandayasi, J. Phys. Soc. Jpn. **41**, 1879 (1976).
[22] For fields above the transition, the values of A presented here are larger than our previously reported data, which were derived from the resistivity data taken in a downward field sweep (Ref. 12). This is because the current data were fitted in a lower temperature range of <3 K, while the previous data were fitted in the range of 5–12 K.